A novel PET tracer 18F-deoxy-thiamine: synthesis, metabolic kinetics, and evaluation on cerebral thiamine metabolism status

Changpeng Wang
Zhongshan Hospital Fudan University
Siwei Zhang
Jiangsu Huayi Technology Co., Ltd., Jiangsu
Yuefei Zou
Jiangsu Huayi Technology Co., Ltd., Jiangsu
Hongzhao Ma
Jiangsu Huayi Technology Co., Ltd., Jiangsu
Donglang Jiang
Huashan Hospital Fudan University
Lei Sheng
Zhongshan Hospital Fudan University
Shaoming Sang
Zhongshan Hospital Fudan University
Lirong Jin
Zhongshan Hospital Fudan University
Yihui Guan
Huashan Hospital Fudan University
Yuan Gui
Jiangsu Huayi Technology Co., Ltd., Jiangsu
Zhihong Xu
Jiangsu Huayi Technology Co., Ltd., Jiangsu
Chunjiu Zhong (zhongcj@163.com)
Zhongshan Hospital Fudan University

Original research

Keywords: Thiamine,18F-labeled thiamine, tracer,positron emission tomography

Posted Date: July 30th, 2020

DOI: https://doi.org/10.21203/rs.3.rs-28109/v2

Version of Record: A version of this preprint was published on October 20th, 2020. See the published version at https://doi.org/10.1186/s13550-020-00710-5.

Abstract

Background: Some neuropsychological diseases are associated with abnormal thiamine metabolism, including Korsakoff-Wernicke syndrome and Alzheimer's disease. However, *in vivo* detection of the status of brain thiamine metabolism is still unavailable and needs to be developed.

Methods: A novel PET tracer of ^{18}F-deoxy-thiamine was synthesized using an automated module via a two-step route. The main quality control parameters, such as specific activity, radiochemical purity, radiochemical concentration, were evaluated by high performance liquid chromatography (HPLC). Metabolic kinetics and brain level of ^{18}F-deoxy-thiamine in mice and marmosets were studied by micro-positron emission tomography/computed tomography (PET/CT). *In vivo* stability, renal excretion rate, biodistribution of ^{18}F-deoxy-thiamine in the mice were assayed using HPLC and γ-counter. Also, the correlation between the retention of cerebral ^{18}F-deoxy-thiamine in 60 minutes after injection as represented by the area under the curve (AUC) and blood thiamine levels were investigated.

Results: The ^{18}F-deoxy-thiamine was stable both *in vitro* and *in vivo*. The uptake and clearance of ^{18}F-deoxy-thiamine were quick in the mice. It reached the max standard uptake value (SUVmax) of 4.61±0.53 in the liver within 1 minute, 18.67±7.04 in the kidney within half a minute. The SUV dropped to 0.72±0.05 and 0.77±0.35 after 60 minutes of injection in the liver and kidney, respectively. After injection, kidney, liver, and pancreas exhibited high accumulation level of ^{18}F-deoxy-thiamine, while brain, muscle, fat, and gonad showed low accumulation concentration, consistent with previous reports on thiamine distribution in mice. Within 90 minutes after injection, the level of ^{18}F-deoxy-thiamine in the brain of C57BL/6 mice with thiamine deficiency by thiamine-deprived diet (TD) was 1.9 times higher than that in control mice, and was 3.1 times higher in ICR mice with TD than that in control mice. The AUC of the tracer in the brain of marmosets within 60 minutes was 29.33 ± 5.15 and negatively correlated with blood thiamine diphosphate levels ($r = -0.985$, $p = 0.015$).

Conclusion: The ^{18}F-deoxy-thiamine meets the requirements for ideal PET tracer for *in vivo* detecting the status of cerebral thiamine metabolism.

Introduction

Thiamine, also named vitamin B_1, is an essential nutrient that can be acquired only via diet. After being absorbed from gastrointestinal tract, thiamine is delivered to all organs and tissues and converted into bioactive thiamine diphosphate (TDP) [1]. Thiamine deficiency (TD) is associated with some neuropsychological diseases, such as Wernicke–Korsakoff syndrome, Alzheimer's disease (AD), beriberi, Leigh syndrome, and so forth, and results in lactic acidosis, mitochondrial dysfunction, and energy deficits in brain, muscle, and heart, causing a broad range of clinical manifestations, such as anorexia,

agitation, diminished tendon reflexes, ataxia, disturbance of consciousness, muscle pain, and heart failure, etc. [2-4]

Glucose is the predominant substrate of brain energy metabolism and plays a pivotal role in maintaining cerebral function [5], which makes the brain vulnerable to glucose dysmetabolism. TDP is the common coenzyme of the three key enzymes in glucose catabolism: pyruvate dehydrogenase and α-ketoglutarate dehydrogenase in the Krebs cycle that is responsible for producing ATP in mitochondria, and transketolase in pentose phosphate pathway that generates antioxidants and the substrates of biosynthesizing DNA, RNA, and fatty acid in cytosol [6]. Therefore, the brain also is susceptible to TD by disturbing glucose metabolism [2, 7-12]

However, *in vivo* detection of cerebral thiamine metabolism status is still unavailable. In this study, a novel radiotracer of positron emission topography (PET)—^{18}F-deoxy-thiamine was designed and synthesized (Figure 1) and its metabolic kinetics was studied. The retention of ^{18}F-deoxy-thiamine in the brains of mice and marmosets was studied.

Materials And Methods

1. **General information**

All reagents were purchased from TCI Development Co., Ltd (Shanghai) and J & K Scientific (Beijing, China) unless otherwise indicated. Thin layer chromatography (TLC) was performed with silica gel layers, and compounds were visualized under UV light. The ^{1}H NMR (300 MHz) spectra of all compounds were acquired on an Advance (Bruker) spectrometer. Chemical shifts (δ) for the proton resonance were reported in parts per million (ppm) downfield from TMS (δ = 0). The identification and purity of precursors as well as cold standard sample were determined by a LC-MS instrument (1200/6120, Agilent Technologies Inc.) with a C_{18} column (4.6 * 150mm 5uM; VP-ODS, Shimadzu) at 0.5 ml per minute (ml/min) flow rate. The mobile phase consisted of 60% methanol and 40% H_2O containing millesimal formic acid.

^{18}F ions were obtained from a cyclotron (Cyclone 18 Twin, IBA, Belgium), situated at the Molecular Imaging institute, Jiangsu Huayi Technology Co., Ltd., by the nuclear reaction [^{18}O(p,n)^{18}F]. For automatic synthesis of ^{18}F-deoxy-thiamine, we used a remote-controlled radiolabeling module (RNplus, Synthra) with slight modifications and created the sequence program, based on manual trials. The scheme of modified RNplus module is presented in Supplementary Figure 1. We used six reagent supply vials (A1-A5, B1) at the upper part and two reaction vials (vial I and vial II) at the bottom part.

Analytical HPLC (1260, Agilent Technologies Inc.) with the same type of column mentioned above was employed for ^{18}F-deoxy-thiamine characterization and identification. The signal acquisition system

consisted of a UV detector (254 nm) and a radio-detector (1IINaI/PMT, Lablogic, USA) in series. The flow rate was 0.8 ml/min and the mobile phase consisted of methanol and H_2O containing 0.05% triethylamine and 50mM ammonium acetate. The percentage of methanol/H_2O changed with running time: 0-15 minutes (mins), 15%/85%; 15-25 mins, methanol increasing to 100% while H_2O decreasing to 0%; 25-30 mins, methanol 100%.

A micro-PET/CT equipment (Inveon; Siemens Co., USA) was used for detecting the levels of ^{18}F-deoxy-thiamine in the organs of mice and marmosets. During micro-PET/CT scanning, the body temperature of mice and marmosets was maintained at 37°C using a heat pad.

C57BL/6 and Institute of Cancer Research (ICR) mice (obtained from the SLAC Laboratory Animal Company, China) were housed in a controlled environment at temperature of 20-26 ^{o}C and humidity of 40-70% with free access to food and water. The marmosets were supplied by Jiuting Non-human Primate Facility, Chinese Academy of Sciences, Shanghai. Four marmosets aged 3.1-10.8 years old were employed for micro-PET/CT scanning (M1: 3.1y, female; M2: 3.5y, male; M3: 5.4y, female; M4: 10.8y, male). At the day of experiment, the marmosets were fetched from the facility, and were sent back when the scanning finished.

All animal care and experimental procedures were carried out according to the guidelines of the Animal Care Committee of Fudan University. This study was approved by Medical Experimental Animal Administrative Committee of Fudan University, and the committee on medical ethics of Zhongshan Hospital, Fudan University.

2. **Synthesis of cold standard sample of ^{18}F-deoxy-thiamine as well as precursors (5) and (6).**

We synthesized cold standard sample of ^{18}F-deoxy-thiamine as well as precursors (5) and (6) according to the work of Cline JK, et al.[13], with minor modifications (Supplementary Figure 2). The purity of the standard sample is > 99.9%, and the purity of two precursors > 99%, identified via HNMR and LC-MS (Supplementary Figure 3B-G). The details of the synthetic route were described in the Supplementary text.

3. **Automated radiosynthesis of ^{18}F-deoxy-thiamine**

We adopted a two-step synthesis route (Figure 1). The scheme of automated synthesis was shown in Supplementary Figure 1. Reagents were added into supply vials as follows: A1: 1.1 ml eluent (3.08 mg $KHCO_3$, 11 mg Kryptofix 2.2.2, 0.88 mL MeCN, 0.22 mL H_2O); A2: 1 ml MeCN; A3: 5 mg precursor **(6)** in 0.5 ml MeCN; A4: 1 ml MeCN; A5: 0.5 ml MeCN; B1: 0.5 ml H_2O. 5 mg precursor **(5)** powder was also added into reaction vial II beforehand. When the first step synthesis finished, the intermediate product [^{18}F]-compound **(7)** was transferred from reaction vial I to reaction vial II via distillation. The whole automated

synthesis duration was 100 mins. The details of synthesis and purification were described in the Supplementary text.

4. **Characteration and quality control of ^{18}F-deoxy-thiamine**

Radiochemical yield (RCY, decay-correction to the end of bombardment) and radiochemical concentration (RCC) were measured by the radioactivity calibrator (CRC-55tR, CAPINTEC, INC., USA). ^{18}F-deoxy-thiamine was identified by co-injecting final product with cold standard sample into analytical HPLC. Radiochemical purity (RCP) and specific radioactivity (SA) were calculated by means of the area under curve (AUC) of radio-signals and UV-signals of final product in analytical HPLC, respectively. Bacteria and endotoxin detections were carried out by means of anaerobic/aerobic bacteria media and Limulus reagent gel methods, respectively, according to Chinese Pharmacopoeia.

5. ***In vitro* stability**

^{18}F-deoxy-thiamine solution was stored at room temperature (RT) and injected into analytical HPLC for evaluating RCP and peak shape at 0 hour (h), 2h, 4h, 6h, 8h, and 10h, respectively after synthesized.

6. **Thiamine deficiency mouse model**

Eight-week-old male C57BL/6 and ICR mice were randomly divided into two groups: TD mouse models (n = 2 for C57BL/6, one died due to anesthesia during micro-PET/CT scanning; n = 3 for ICR) were established by feeding thiamine-deprived diet (Trophic Animal Feed High-tech Co., Ltd., China). Control mice (n=3 for each strain) were fed the general diet. Twenty-eight days later, all mice received PET/CT scanning.

7. **Micro-PET/CT imaging**

Micro-PET/CT imaging using ^{18}F-deoxy-thiamine as the tracer was performed in the mice with TD and control mice, as well as in marmosets. The animals were anesthetized by inhaling 1.5%-2% of isoflurane in air (1.5 L/min) and received CT scan for acquiring structure image and attenuation correction data. Then, the mice were injected with 7.4-14.8 MBq of ^{18}F-deoxy-thiamine in 0.1ml volume (diluted by normal saline) through the tail vein. Brain PET imaging was immediately performed and dynamically acquired for 90 mins with an energy window of 350-650KeV and a time window of 3.438 ns. A total of 35 frames were setup: 20f, 3s; 4f, 60s; 5f, 300s; 6f, 600s. Dynamic images were reconstructed by OSEM3D/SP-MAP algorithm with two iterations. After scanning, the mice were sacrificed. The blood samples of the mice

were taken from cardiac ventricle for measuring the levels of thiamine, thiamine monophosphate (TMP), and TDP.

The marmosets were injected with 46.3-74.0 MBq of ^{18}F-deoxy-thiamine in 0.5-0.8 ml volume through the femoral vein. Brain PET imaging was immediately scanned and dynamically acquired for 60 mins. A total of 18 frames was setup: 6f, 10s; 4f, 60s; 5f, 300s; 6f, 600s. The blood samples of the marmosets were taken from femoral vein for measuring the levels of thiamine, TMP, and TDP. The other conditions for marmosets were the same as that for mice.

Regions of interest (ROIs) were drawn manually over the whole brain (for mice and marmosets) and in the left ventricular cavity (for marmosets) based on the PET/CT co-registered images using IRW 4.2 software (Siemens Medical Solutions USA, Inc.). Radioactivity was expressed as standard uptake value (SUV): (ROI radioactivity/ROI volume)/(injected radioactivity/gram of body weight). The time-activity curve (TAC) and AUC (SUV*mins) were also calculated.

The TACs of the marmosets blood (Radioactivity was expressed as SUV) were taken as input functions (IF) [14-16] for fitting Patlak plots [17, 18], in order to analyze transfer constants (K_i) of brains in marmosets (IRW 4.2 software). The details of Patlak model was described in the supplemental text.

8. **Measurement of thiamine, TMP, and TDP in whole blood samples of mice and marmosets**

Thiamine, TMP, and TDP levels in whole blood samples were measured using HPLC, based on the established mothed [4] with slight modification. Briefly, blood samples were collected using heparin-anticoagulated tubes, 150 ul sample was vibrated for 30s with equal volume 5.7% (for mice) or 5.2% (for marmosets) perchloric acid (PCA) added dropwise for deproteinization. Then, the mixture was stored at -80^{o}C until assay within one month. The mixture was centrifuged at 12000 rpm for 8 mins at 4 ^{o}C, the supernatant was pipetted. Thiamine, TMP, and TDP in supernatant were derivatized into thiochromes using potassium ferricyanide and analyzed by gradient elusion with C_{18} reversed-phase analytical column (250 X 4.6 mm). The derivatives were identified by HPLC fluoroscopy (1100, Agilent Technologies Inc., ex: 367nm, em: 435nm). The thiamine, TMP, and TDP levels were quantified using standard samples (Sigma-Aldrich, St. Louis, MO). The analyzers were blinded to samples information.

9. **Studies of pharmacokinetic and metabolic kinetics in liver and kidney of mice**

Nine-week-old male ICR mice (n=5) were dynamically scanned using micro-PET/CT for 60 mins. A total of 18 frames was reconstructed: 6f, 10s; 4f, 60s; 5f, 300s; 6f, 600s. The scanning conditions were the same as that mentioned above. The ROIs of liver and renal parenchyma as well as left ventricular cavity were manually drawn.

For pharmacokinetic study, the TACs of the blood were fitted. The radioactivity was evaluated as %IA/g (the percentage of injected activity per gram of blood). Pharmacokinetics parameters were counted through the software PKSolver (version 2.0, China Pharmaceutical University) [19].

For metabolic kinetics study, SUV, TAC, AUC, maximum radioactivity (C_{max}), and time to C_{max} (T_{max}) were calculated. The TACs of the blood (Radioactivity expressed as SUV) were taken as IFs for fitting Logan plots [20, 21], in order to analyze the distribution volumes (V_D) of ^{18}F-deoxy-thiamine in liver and kidney, respectively (IRW 4.2 software). The details of Logan model were described in the supplemental text.

10. Biodistribution study

The biodistribution of ^{18}F-deoxy-thiamine was studied in ICR mice (n = 36 in total; 18 males, nine-weeks-old, 33.5 ± 4.0 g; 18 females, seven-week-old, 27.7 ± 5.0 g). For each mouse, 0.1 ml of ^{18}F-deoxy-thiamine solution (37 MBq/ml) was injected into the tail vein under isoflurane anesthesia. The mice were sacrificed at 5 mins, 10 mins, 30 mins, 1 h, 2 hs, and 4 hs after injection (3 males and 3 females for each time point). The tissues of heart, liver, spleen, lung, kidney, stomach, duodenum, pancreas, femur, muscle (from thigh), artery blood, brain, fat, and gonad (ovary or testicle) were harvested, weighted, and measured for radioactivity by γ-counter. %IA/g was calculated referring to the counts of standard samples.

11. *In vivo* stability and the renal excretion rate

After metabolic kinetics study (Heading 9, Materials and Methods section), the mice were stop to exposure to isoflurane and woke up several mins later. The urine accumulated in the bladder of the mice during the whole anesthetization period would be excreted. Some mice were softly rubbed the lower bowel in order to promote urination. The duration from the injection of ^{18}F-deoxy-thiamine to mouse urination was about 85 mins. The urine samples from three ICR mice were collected using syringes and measured in the radioactivity calibrator. Then, 0.1 ml urine for each mouse was added in an Eppendorf tube, vibrated for 30s with equal volume PCA added dropwise for deproteinization. After centrifuging at 12000 rpm for 8 mins at 4 ^{o}C, the supernatant was filtered and analyzed using HPLC.

12. Statistical analysis

For the continuous data, mean ± standard error of mean (SEM) was applied for statistical description. Student *t* test was employed to compare the AUC values between TD mice and controls in ICR strain. The Pearson correlation was utilized to analyse the correlation between the cerebral accumulation of ^{18}F-deoxy-thiamine and the levels of blood thiamine, TMP, and TDP in marmosets. Repeated measurement of

ANOVA with Trukey's *post-hoc* was used to analyse the AUC values of ^{18}F-deoxy-thiamine in brain, liver, and kidney in ICR mice. All statistical analyses were performed using SPSS (Statistical Package for the Social Sciences) software (version 22.0; SPSS Inc., Chicago IL).

Results

1. **Characteration and quality control of ^{18}F-deoxy-thiamine**

The solution of ^{18}F-deoxy-thiamine was clear and free of particles with the naked eye[18]. All relevant items of characterization were shown in Table 1. The RCP and SA were 98.28±0.39% and > 55.5 GBq/umol, respectively (Figure 2). The RCY was 5.17±1.04% (decay-corrected to the end of bombardment), and the RCC was 740-1110 MBq/ml. The bacteria and endotoxin tests were negative. For exploring the expiration time, we tested the stability *in vitro*. ^{18}F-deoxy-thiamine final product was stable at RT, with the RCP > 95% six hours, and > 93% ten hours after synthesis (Table 2).

2. **Evaluation of cerebral thiamine metabolism status**

2.1. C57BL/6 mice

The cerebral retention of ^{18}F-deoxy-thiamine was increasing and approached to C_{max} at the terminal time of 90 mins in the two mice with TD. The $SUVs_{max}$ of the last frame (80-90 min) were 0.48 (TD 3 mouse) and 0.55 (TD 5 mouse). The AUC values within 90 mins were 34.99 (TD 3 mouse) and 42.46 (TD 5 mouse). In contrast, the cerebral retention was stable within 90 mins in the three control mice, the $SUVs_{max}$ were about 0.17 (Ctrl 2 mouse), 0.25 (Ctrl 4 mouse), and 0.3 (Ctrl 1 mouse). The AUC values within 90 mins were 14.52 (Ctrl 2 mouse), 20.96 (Ctrl 4 mouse), and 25.67 (Ctrl 1 mouse) (Figure 3A-B). The mean of AUC values in TD mice was 1.9 times higher than that in control mice (38.73±3.74 vs. 20.38±3.23).

2.2. ICR mice

The values of cerebral $SUVs_{max}$ in three mice with TD were 0.98 at 28th frame (TD 3 mouse, 20-25 min), 0.97 at 30th frame (TD 4 mouse, 30-40 min), and 0.61 at the 33th frame (TD1 mouse, 60-70 min) and then the SUVs declined slowly. The AUC values within 90 mins were 79.28 (TD 3 mouse), 78.75 (TD 4 mouse), and 46.81 (TD 1 mouse), respectively. The $SUVs_{max}$ of ICR control mice were 0.36 (Ctrl 1 mouse), 0.27 (Ctrl 5 mouse), and 0.18 (Ctrl 3 mouse) within 90 mins, respectively. The TACs in control mice were stable, similar to that in the C57BL/6 strain mice. The AUC values within 90 mins were 29.58 (Ctrl 1 mouse), 21.14 (Ctrl 5 mouse) and 14.92 (Ctrl 3 mouse), respectively (Figure 3C-D). The mean of AUC values in TD mice was 3.1 times higher than that in controls (68.28 ± 10.74 vs. 21.88 ± 4.25, P = 0.016).

2.3. Marmosets

The retention of ^{18}F-deoxy-thiamine in the cerebrum of three marmosets had been increasing within 60 mins (M1, M3, M4), and reached plateau at 16th frame (30-40 min) in M2. The values of SUV_{max} were between 0.33 to 0.90, and the AUC values within 60 mins were between 17.07 to 42.28 (29.33±5.15; Figure 3E-F). There was a significantly negative correlation between cerebral AUC values within 60 mins and TDP levels in whole blood samples (r = -0.985, p = 0.015, Figure 3I). No significant correlation was found between the AUC values of ^{18}F-deoxy-thiamine in cerebrum and blood thiamine and TMP levels (Figure 3G-H). In order to quantitatively evaluate the uptake of ^{18}F-deoxy-thiamine in the cerebrum of marmosets, the Patlak model was utilized to analyze the blood-to-brain transfer rate represented by constant K_i based on the characteristics of metabolic kinetics in the brain. The regression plots were fitted automatically by software from 20 min to 60 min. K_i was between 0.0030-0.0102 ml/g/min, and significantly correlated with age (r = 0.986, P = 0.014, Figure 3J, see the fitted Patlak plots in Supplementary Figure 4).

3. Pharmacokinetic study and metabolic kinetics study in liver and kidney of mice

Table 3 showed the pharmacokinetic parameters. Figure 4A showed the TAC of ^{18}F-deoxy-thiamine (radioactivity as IA%/g) within 60 mins in the ICR mice blood represented by the ROI in left ventricle. The pharmacokinetic profiles of ^{18}F-deoxy-thiamine fitted a two-compartment open model. The value of $AUC_{0-60\ min}$ was 37.313, accounting for 99.77% of the value of AUC_{0-inf} (37.399), which implies that the 60 mins observation be sufficient to depict the pharmacokinetic characters. The T_{max} was in the first frame (0-10 sec) and the C_{max} was 18.12 ± 2.20 IA%/g, respectively. The half-life of distribution ($t_{1/2\alpha}$) and half-life of elimination ($t_{1/2\beta}$) were 0.082 and 6.379 mins. The volume of distribution (V_D1) and clearance rate (CL1) of central compartment were 3.058 g and 2.674 g/min. The V_D2 and CL2 of peripheral compartment were 19.308 g and 20.162 g/min. These results revealed that ^{18}F-deoxy-thiamine could be absorbed and eliminated rapidly.

The representative images of dynamic micro-PET/CT whole-body scanning of ICR mice within 60 mins were shown as the Figure 5. Initially, ^{18}F-deoxy-thiamine distributed mainly into liver and bladder. Then, the radioactivities in the liver quickly declined while that in bladder was increasing over time. These results demonstrated that the uptake and elimination of ^{18}F-deoxy-thiamine *in vivo* were fast and mainly occurred in liver and kidney.

The T_{max} in liver was approximately 1 min post injection. The value of SUV_{max} was 4.61±0.53. Then, the SUV dropped fast to 3.23±0.50 at approximately 5 min. The radioactivity continued to declined afterwards. The SUV was 0.72±0.05 at the terminal time (60 mins). The AUC value within 60 mins was 79.94±5.43 (Figure 4B). The T_{max} in the kidney were approximately 30 seconds (secs), and the SUV_{max}

was 18.67±7.04. The SUV dropped fast to 3.29±0.50 in 10 mins, and continued to drop slowly. At the terminal time (60 mins), the SUV dropped to 0.77±0.35. The AUC value was 113.4±15.56 (Figure 4C). The AUC values of liver and kidney within 60 mins were significantly higher than that of whole brain ($P < 0.001$). Also, the AUC values in kidney were significantly higher than that in liver ($P < 0.05$, Figure 4D).

Logan plot was applied to analyze the distribution volume (V_D) of liver and kidney based on the characteristics of metabolic kinetics. The regression plots were fitted automatically by software from 10 min to 60 min, and V_D were 4.573±0.34 ml/g in the liver and 6.17±0.88 ml/g in the kidney (Supplementary Figure 5A-E, 6A-E). The results indicated that the “steady-state” of uptake/clearance was reached in the 10^{th} min, and the mean uptake amount of ^{18}F-deoxy-thiamine per gram tissue was equivalent to the amount contained in 4.573 ml (for liver) or 6.17 ml (for kidney) of blood.

4. ***In vivo* stability and renal excretion rate**

Since the -OH group of thiamine is replaced by -^{18}F, ^{18}F-deoxy-thiamine cannot enter the known metabolic pathways of thiamine till ^{18}F decays back to $^{18}O^-$ [22, 23]. We collected about 0.1ml urine per ICR mouse about 85 min after tail vain injection. The radioactivity in urine was 34.16±3.84% of total injected radioactivity measured by radioactivity calibrator (decay-correction), and no correlation was found between the excreted radioactivity in urine and the injected radioactivity (Supplementary Table 1). The RCP of renal excreted ^{18}F-deoxy-thiamine was 94.53 ± 0.81% determined by HPLC. In addition, an unknown trace substance (3.30 ± 0.60% in RCP) was found ahead of ^{18}F-deoxy-thiamine, which could not be $^{18}F^-$ ions according to its retention time and shape (Figure 6). The percentage of intact tracer was 96.63%. These results indicated that about one third of ^{18}F-deoxy-thiamine was excreted by kidney and that ^{18}F-deoxy-thiamine was stable within 85 mins *in vivo*.

5. **Biodistribution study**

As a derivative of an essential vitamin, ^{18}F-deoxy-thiamine distributed widely *in vivo*. In most of the organs and tissues of ICR mice, the C_{max} of ^{18}F-deoxy-thiamine achieved between 5 to 15 mins, then ^{18}F-deoxy-thiamine was cleared rapid and the accumulation was very low in these organs and tissues till 4 hours after injection (Figure 7, Supplementary Table 2). The muscular radioactivity in female ICR mice began to decline 5 mins after injection, differentiating from that in male ICR mice, in which the radioactivity increased within 60 mins, then declined rapid.

Consistent with the results of PET/CT scanning, liver and kidney were the main distribution organs. The biodistribution of ^{18}F-deoxy-thiamine in brain, fat, and gonad was less than the observed other organs or

tissues. Interestingly, the level of ^{18}F-deoxy-thiamine in the ovary was higher than that in the testicle, indicating the difference in ^{18}F-deoxy-thiamine metabolism between male and female gonads.

Discussion

The levels of thiamine and its phosphate esters decline in the brains of mice with TD [24]. Our current study showed the retention of ^{18}F-deoxy-thiamine was higher in the cerebra of two strains mice with TD as compared with that in control mice (Figure 3 A-D). The results indicate that the enhanced accumulation of ^{18}F-deoxy-thiamine in the brain could reflect the status of cerebral thiamine deficiency of the mice. It may be due to the fact that brain elevates the uptake efficiency of thiamine from periphery blood in order to meet the demands of high rate of glucose metabolism as well as other thiamine-dependent physiological activities under the condition of thiamine deficiency. TDP accounts for 90% of total thiamine in the body [25]. We observed that the level of ^{18}F-deoxy-thiamine in the brain significantly negatively correlated with blood TDP levels in marmosets (Figure 3I). In addition, the blood-to-brain transfer rate as represented by K_i was significantly positively correlated with the age of marmosets (Figure 3J), suggesting that the reserve of thiamine in marmosets declines with age. The result is consistent with our previous observation in the non-demented elderly [26]. Of course, this result should be further validated by expanding the sample size in future studies.

The previous study has showed that TDP reduction contributes to cerebral glucose hypometabolism of AD, and the concentration of blood TDP was positively correlated with the level of cerebral glucose metabolism in AD patients [24]. Cerebral glucose metabolism is extremely high, which under normal circumstances, the brain glucose concentration is kept constant at the millimole concentration and cerebral metabolic rate of glucose (CMR_{Glu}) reaches 0.2-0.3umol/g/min [27, 28]. It may lead to the possibility that slight alteration of brain glucose metabolism under some pathological conditions is difficult to be detected by PET with [^{18}F]-fluorodeoxyglucose (FDG-PET). In this study, the SUVs of ^{18}F-deoxy-thiamine in the brains of control mice and marmosets were less than 0.4 and 0.9, respectively (Figure 3A and C). It is much lower than that of FDG in the range of 1 to 2 in the brains of mice [29]. The results imply that PET with ^{18}F-deoxy-thiamine may be more sensitive than FDG-PET for evaluation of mild brain hypometabolism status. The advantages and disadvantages of these two methods for detecting brain metabolic status should be further investigated in future studies.

In both genders of ICR mice, kidney, liver, and pancreas exhibit high accumulation level of ^{18}F-deoxy-thiamine, while brain, muscle, fat, and gonad show low accumulation concentration (Figure 7; Supplementary Table 2, 3). These results are consistent with previous reports on the biodistributions of thiamine and its phosphate esters [29-31]. Besides, we found that 3.37% of ^{18}F-deoxy-thiamine in urine was metabolized to more polar compounds after 85 mins *in vivo* process (Figure 6). To our knowledge, the –OH group is the active site for thiamine converting into bioactive TDP *in vivo* [22, 23]. Thus, before -^{18}F decays back to stable isotope -^{18}O, ^{18}F-deoxy-thiamine could not enter the known metabolic routes.

The presence of this 3.37% compounds implied other unknown metabolic routes might exist. ^{18}F-deoxy-thiamine could help for further exploration on the metabolism and biodistribution of thiamine.

Stability is important for PET tracer. ^{18}F-deoxy-thiamine was stable at RT. The RCP was > 95% 6h, and > 93% 10h after synthesis, which means no significant radiolysis effect exists *in vitro* (Table 2) [32]. In addition, no ^{18}F-deflourination of ^{18}F-deoxy-thiamine *in vivo* was observed based on the phenomenon that the accumulation of radioactivity signal in bone was decreasing over time [34] (Figure 7 B and E). Also, the prototype form of ^{18}F-deoxy-thiamine excreted in urine reached 96.63% within 85 mins after vein injection (Figure 6). These results demonstrated ^{18}F-deoxy-thiamine was highly stable both *in vitro* and *in vivo*.

Pharmacokinetic and metabolic kinetics studies as well as biodistribution study indicated that the uptake and clearance of ^{18}F-deoxy-thiamine *in vivo* were fast, which is another important requirement. The $t_{1/2\beta}$ was 6.379 mins, CL_1 and CL_2 were 2.674 g/min and 20.162 g/min, respectively (Table 3). The values of C_{max} in various tissues and organs of ICR mice reached within 15 mins (except for muscle of males, reached within 1h), and the accumulation of ^{18}F-deoxy-thiamine was very low in these tissues and organs till 4 hours after injection (Figure 7, Supplementary Table 2 and 3). Besides, about one third of ^{18}F-deoxy-thiamine was excreted through kidney 85 mins after injection (Supplementary Table 1).

Graphical analysis technique has been extensively applied in the analyses of nuclear medicine imaging data. It is especially suitable for pharmacokinetic studies of novel tracers before the compartmental models are fully described, because it is independent of any specific model configuration [21]. We analyzed the important kinetic parameters K_i and V_D in the brain of marmosets and in the liver and kidney of ICR mice employing Patlak and Logan plots, respectively, based on the characteristics of TACs in these organs (Figure 3E, Figure 4B, C). The V_D in the kidney and liver of ICR mice were 6.17±0.88 ml/g and 4.573±0.34 ml/g, respectively. The results showed that the uptake and clearance of ^{18}F-deoxy-thiamine *in vivo* were fast.

Thiamine consists of a pyrimidine ring with an electronegative amidogen and a thiazole ring. The structural complexity determines the difficulty of artificially synthesizing and modifying thiamine. Since the first synthesis route was reported in 1937 [13], only a few studies on thiamine synthesis and modification have been published [35-37]. Recently, Doi H, et al. synthesized radio-labelled thiamine with ^{11}C [37], and conducted heart imaging study in rats [38]. Although ^{11}C-thiamine possesses the same molecular structure as thiamine itself, the short half-life of ^{11}C (20.4 mins) limits its application. Also, ^{11}C-thiamine would be phosphorylated to ^{11}C-TDP fast via the -OH group *in vivo* [38], which complicates the interpretation of the radio-signal. Here, ^{18}F-deoxy-thiamine was successfully synthesized by a two-step route, in which -OH group of thiamine replaced by -^{18}F (Figure 1). Although the RCY was not high enough, the RCP, SA and RCC were high (Table 1). The bacteria and endotoxin tests were negative. These results indicated that ^{18}F-deoxy-thiamine was safe and suitable for *in vivo* studies.

The most difficult part in our two-step route is the isolation and purification of the intermediate product ^{18}F-compound **(7)**. Though we have tried various solid phase extractions as well as preparative HPLC, either the isolation failed or the process became too complicated to be automated. The molecule of 4-methyl-5(beta-hydroxyethyl)-thiazole is solid, and its boiling point is 135^{o}C under vacuum [39]. Once -OH is changed to -F, however, this compound becomes oil and volatile at RT. We speculated that it was because the H bond connecting H and N was broken (Supplementary Figure 7). By distillation, we successfully isolated compound **(7)** and realized the automation of the radiosynthesis route.

Conclusion

In this study, we synthesized a novel PET tracer of ^{18}F-deoxy-thiamine and established its automated synthesis route. Further, ^{18}F-deoxy-thiamine was stable *in vitro* and *in vivo*, and possessed ideal characteristics of metabolic kinetics. The PET with ^{18}F-deoxy-thiamine could evaluate the status of cerebral thiamine metabolism, and might be more suitable for evaluating cerebral energy metabolism than FDG-PET due to the low abundance of cerebral thiamine metabolism. However, the sample size of marmosets in this study was not large enough, and we lack of TD model of marmosets to further investigate thiamine metabolism in non-human primates. This study laid the foundation for further studies on diseases related to thiamine dysmetabolism.

Declarations

Ethical approval

All animal care and experimental procedures were carried out according to the guidelines of the Animal Care Committee of Fudan University. This study was approved by Medical Experimental Animal Administrative Committee of Fudan University, and the committee on medical ethics of Zhongshan Hospital, Fudan University.

Consent for publication

Not applicable.

Availability of data and materials

The datasets used in the current study are available from the corresponding author on reasonable request.

Conflict of interest

Chunjiu Zhong holds shares of Shanghai Rixin Biotech Co., Ltd., which focuses on the development of new drugs against Alzheimer's disease. The other authors declare that he/she has no conflict of interest.

Funding

This study was financially supported by the National Key Research and Development Program Foundation of China (2016YFC1306403) to Chunjiu Zhong, the National Natural Science Foundation of China (grant no. 91332201) to Chunjiu Zhong, and Zhongshan Hospital Science Foundation (2018ZSQN28) to Changpeng Wang.

Authors' contributions

Zhong C conceived the study. Zhong C and Wang C designed the study. Wang C, Zhang S, Zhou Y, Ma H, Gui Y and Xu Z were responsible for radiosynthesis. Wang C, Jiang D, Sheng L, Sang S, Jin L, and Guan Y was responsible for animal studies. The manuscript was drafted by Wang C and Zhong C. All authors read and approved the final manuscript.

Acknowledgements

We thank Profess Fengling Qing, Profess Xiuhua Xu, and Doctor Zenghao Chen for their assistance in synthesis routes.

Abbreviations: thiamine diphosphate, TDP; thiamine monophosphate, TMP; Thiamine deficiency, TD; pentose phosphate pathway, PPP; Thin layer chromatography, TLC; parts per million, ppm; ml per minute, ml/min; radiochemical yield, RCY; radiochemical concentration, RCC; radiochemical purity,

RCP; specific radioactivity, SA; area under curve, AUC; room temperature, RT; region of interest, ROI; standard uptake value, SUV; time-activity curve, TAC; input function, IF; transfer constants, Ki; perchloric acid, PCA; distribution volume, VD; standard error of mean, SEM; clearance rate, CL.

References

1. Talwar D, Davidson H, Cooney J, St JD. Vitamin B(1) status assessed by direct measurement of thiamin pyrophosphate in erythrocytes or whole blood by HPLC: comparison with erythrocyte transketolase activation assay. Clin Chem. 2000;46:704-710.
2. Dhir S, Tarasenko M, Napoli E, Giulivi C. Neurological, Psychiatric, and Biochemical Aspects of Thiamine Deficiency in Children and Adults. Front Psychiatry. 2019;10:207.
3. Hiffler L, Rakotoambinina B, Lafferty N, Martinez GD. Thiamine Deficiency in Tropical Pediatrics: New Insights into a Neglected but Vital Metabolic Challenge. Front Nutr. 2016;3:16.
4. Pan X, Fei G, Lu J, Jin L, Pan S, Chen Z, et al. Measurement of Blood Thiamine Metabolites for Alzheimer's Disease Diagnosis. EBioMedicine. 2016;3:155-162.
5. Bouzier-Sore AK, Voisin P, Bouchaud V, Bezancon E, Franconi JM, Pellerin L. Competition between glucose and lactate as oxidative energy substrates in both neurons and astrocytes: a comparative NMR study. Eur J Neurosci. 2006;24:1687-1694.
6. Butterworth RF, Kril JJ, Harper CG. Thiamine-dependent enzyme changes in the brains of alcoholics: relationship to the Wernicke-Korsakoff syndrome. Alcohol Clin Exp Res. 1993;17:1084-1088.
7. Martin PR, Singleton CK, Hiller-Sturmhofel S. The role of thiamine deficiency in alcoholic brain disease. Alcohol Res Health. 2003;27:134-142.
8. Kril JJ, Harper CG. Neuroanatomy and neuropathology associated with Korsakoff's syndrome. Neuropsychol Rev. 2012;22:72-80.
9. Opdenakker G, Gelin G, De Surgeloose D, Palmers Y. Wernicke encephalopathy: MR findings in two patients. Eur Radiol. 1999;9:1620-1624.
10. Kornreich L, Bron-Harlev E, Hoffmann C, Schwarz M, Konen O, Schoenfeld T, et al. Thiamine deficiency in infants: MR findings in the brain. AJNR Am J Neuroradiol. 2005;26:1668-1674.
11. Jankowska-Kulawy A, Bielarczyk H, Pawelczyk T, Wroblewska M, Szutowicz A. Acetyl-CoA deficit in brain mitochondria in experimental thiamine deficiency encephalopathy. Neurochem Int. 2010;57:851-856.
12. Gibson GE, Blass JP, Beal MF, Bunik V. The alpha-ketoglutarate-dehydrogenase complex: a mediator between mitochondria and oxidative stress in neurodegeneration. Mol Neurobiol. 2005;31:43-63.
13. Cline J K, Williams R R, Finkelstein J. Studies of Crystalline Vitamin B1. XVII. Synthesis of Vitamin B1. Journal of the American Chemical Society. 1937;59:1052-1054.

14. Laforest R, Sharp TL, Engelbach JA, Fettig NM, Herrero P, Kim J, et al. Measurement of input functions in rodents: challenges and solutions. Nucl Med Biol. 2005;32:679-685.
15. Lee YJ, Maeda J, Kusuhara H, Okauchi T, Inaji M, Nagai Y, et al. In vivo evaluation of P-glycoprotein function at the blood-brain barrier in nonhuman primates using [11C]verapamil. J Pharmacol Exp Ther. 2006;316:647-653.
16. Wanek T, Traxl A, Bankstahl JP, Bankstahl M, Sauberer M, Langer O, et al. [(18)F]FDG is not transported by P-glycoprotein and breast cancer resistance protein at the rodent blood-brain barrier. Nucl Med Biol. 2015;42:585-589.
17. Patlak CS, Blasberg RG, Fenstermacher JD. Graphical evaluation of blood-to-brain transfer constants from multiple-time uptake data. J Cereb Blood Flow Metab. 1983;3:1-7.
18. Patlak CS, Blasberg RG. Graphical evaluation of blood-to-brain transfer constants from multiple-time uptake data. Generalizations. J Cereb Blood Flow Metab. 1985;5:584-590.
19. Zhang Y, Huo M, Zhou J, Xie S. PKSolver: An add-in program for pharmacokinetic and pharmacodynamic data analysis in Microsoft Excel. Comput Methods Programs Biomed. 2010;99:306-314.
20. Logan J, Fowler JS, Volkow ND, Wolf AP, Dewey SL, Schlyer DJ, et al. Graphical analysis of reversible radioligand binding from time-activity measurements applied to [N-11C-methyl]-(-)-cocaine PET studies in human subjects. J Cereb Blood Flow Metab. 1990;10:740-747.
21. Logan J. A review of graphical methods for tracer studies and strategies to reduce bias. Nucl Med Biol. 2003;30:833-844.
22. Bettendorff L, Wins P. Thiamin diphosphate in biological chemistry: new aspects of thiamin metabolism, especially triphosphate derivatives acting other than as cofactors. FEBS J. 2009;276:2917-2925.
23. Manzetti S, Zhang J, van der Spoel D. Thiamin function, metabolism, uptake, and transport. Biochemistry. 2014;53:821-835.
24. Sang S, Pan X, Chen Z, Zeng F, Pan S, Liu H, et al. Thiamine diphosphate reduction strongly correlates with brain glucose hypometabolism in Alzheimer's disease, whereas amyloid deposition does not. Alzheimers Res Ther. 2018;10:26.
25. Lu J, Frank EL. Rapid HPLC measurement of thiamine and its phosphate esters in whole blood. Clin Chem. 2008;54:901-906.
26. Lu J, Pan X, Fei G, Wang C, Zhao L, Sang S, et al. Correlation of thiamine metabolite levels with cognitive function in the non-demented elderly. Neurosci Bull. 2015;31:676-684.
27. de Castro IP, Martins LM, Tufi R. Mitochondrial quality control and neurological disease: an emerging connection. Expert Rev Mol Med. 2010;12:e12.
28. Wong KP, Sha W, Zhang X, Huang SC. Effects of administration route, dietary condition, and blood glucose level on kinetics and uptake of 18F-FDG in mice. J Nucl Med. 2011;52:800-807.

29. Klooster A, Larkin JR, Wiersema-Buist J, Gans RO, Thornalley PJ, Navis G, et al. Are brain and heart tissue prone to the development of thiamine deficiency? Alcohol. 2013;47:215-221.
30. Gangolf M, Czerniecki J, Radermecker M, Detry O, Nisolle M, Jouan C, et al. Thiamine status in humans and content of phosphorylated thiamine derivatives in biopsies and cultured cells. PLoS One. 2010;5:e13616.
31. Hilbig R, Rahmann H. Comparative autoradiographic investigations on the tissue distribution of benfotiamine versus thiamine in mice. Arzneimittelforschung. 1998;48:461-468.
32. Jacobson MS, Dankwart HR, Mahoney DW. Radiolysis of 2-[18F]fluoro-2-deoxy-D-glucose ([18F]FDG) and the role of ethanol and radioactive concentration. Appl Radiat Isot. 2009;67:990-995.
33. Chien DT, Szardenings AK, Bahri S, Walsh JC, Mu F, Xia C, et al. Early clinical PET imaging results with the novel PHF-tau radioligand [F18]-T808. J Alzheimers Dis. 2014;38:171-184.
34. Archer S, Perianayagam C. An attempt to apply lethal synthesis to the design of chemotherapeutic agents. Fluorinated 5 beta-(hydroxyethyl)-4-methylthiazoles. J Med Chem. 1979;22:306-309.
35. Lowe G, Potter B V L. Bacteriostatic activity of fluoro-analogues of 5-(2-hydroxyethyl)-4-methylthiazole, a metabolic intermediate in the biosynthesis of thiamine. J. Chem. Soc., Perkin Trans. 1. 1980;2026-2028.
36. Doi H, Mawatari A, Kanazawa M, Nozaki S, Nomura Y, Kitayoshi T, et al. Synthesis of (11)C-Labeled Thiamine and Fursultiamine for in Vivo Molecular Imaging of Vitamin B1 and Its Prodrug Using Positron Emission Tomography. J Org Chem. 2015;80:6250-6258.
37. Nozaki S, Mawatari A, Nakatani Y, Hayashinaka E, Wada Y, Nomura Y, et al. PET Imaging Analysis of Vitamin B1 Kinetics with [(11)C]Thiamine and its Derivative [(11)C]Thiamine Tetrahydrofurfuryl Disulfide in Rats. Mol Imaging Biol. 2018;20:1001-1007.
38. Amos WJ, Neal RA. Isolation and identification of 3-(2'-methyl-4'-amino-5'-pyrimidylmethyl)-4-methylthiazole-5-acetic acid (thiamine acetic acid) and 2-methyl-4-amino-5-formylaminomethylpyrimidine as metabolites of thiamine in the rat. J Biol Chem. 1970;245:5643-5648.

Tables

Table 1. Characteration and Quality Control of ^{18}F-deoxy-thiamine

Items	Results
Physical character	clear and transparent, no macroscopic impurity
pH value	4.5
Alcohols	0%
RCP (n=3)	98.28±0.39%
SA	>55.5 GBq/umol
RCY (n=3)[a]	5.17±1.04%
RCC (n=3)	986.67±123.33 MBq/ml
bacteria test	negative
endotoxin test	negative

a. decay-corrected to the end of bombardment.

Table 2. *In Vitro* Stability Test of ^{18}F-deoxy-thiamine

Time after synthesis (hours)	RCP
0	97.68%
2	96.89%
4	96.11%
6	95.03%
8	94.01%
10	93.38%

Table 3. Pharmacokinetic Parameters of ^{18}F-deoxy-thiamine in ICR Mice (n=5).

Parameters (Units)	Values
T_{max} (s)	0-10
C_{max} (IA%/g)	18.12 ± 2.20[a]
V_D1 (g)	3.058
CL1 (g/min)	2.674
V_D2 (g)	19.308
CL2 (g/min)	20.162
$t_{1/2}(\alpha)$ (min)	0.082
$t_{1/2}(\beta)$ (min)	6.379
AUC $_{0\text{-}60min}$ (%IA/g*min)	37.313
AUC $_{0\text{-}inf}$ (%IA/g*min)	37.399
k_{10} (min^{-1})[b]	0.874
k_{12}(min^{-1})[b]	6.593
k_{21}(min^{-1})[b]	1.044

a. Data were expressed as mean ± SEM.

b. K_{10}, elimination rate constant; K_{12}, elimination rate constant from central compartment to peripheral compartment; K_{21}, elimination rate constant from peripheral compartment to central compartment.

Figures

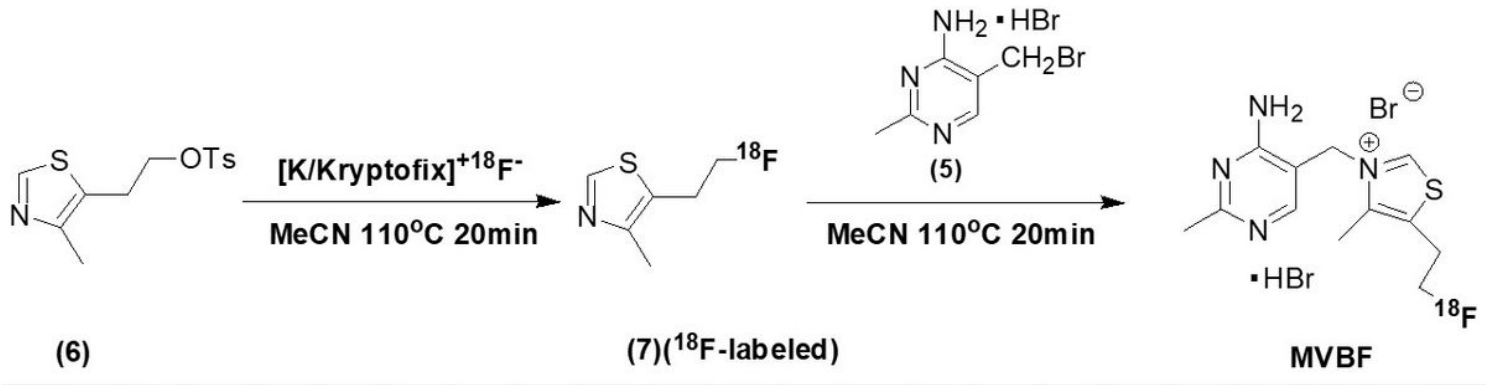

Figure 1

The Two-Step Synthesis of 18F-deoxy-thiamine.

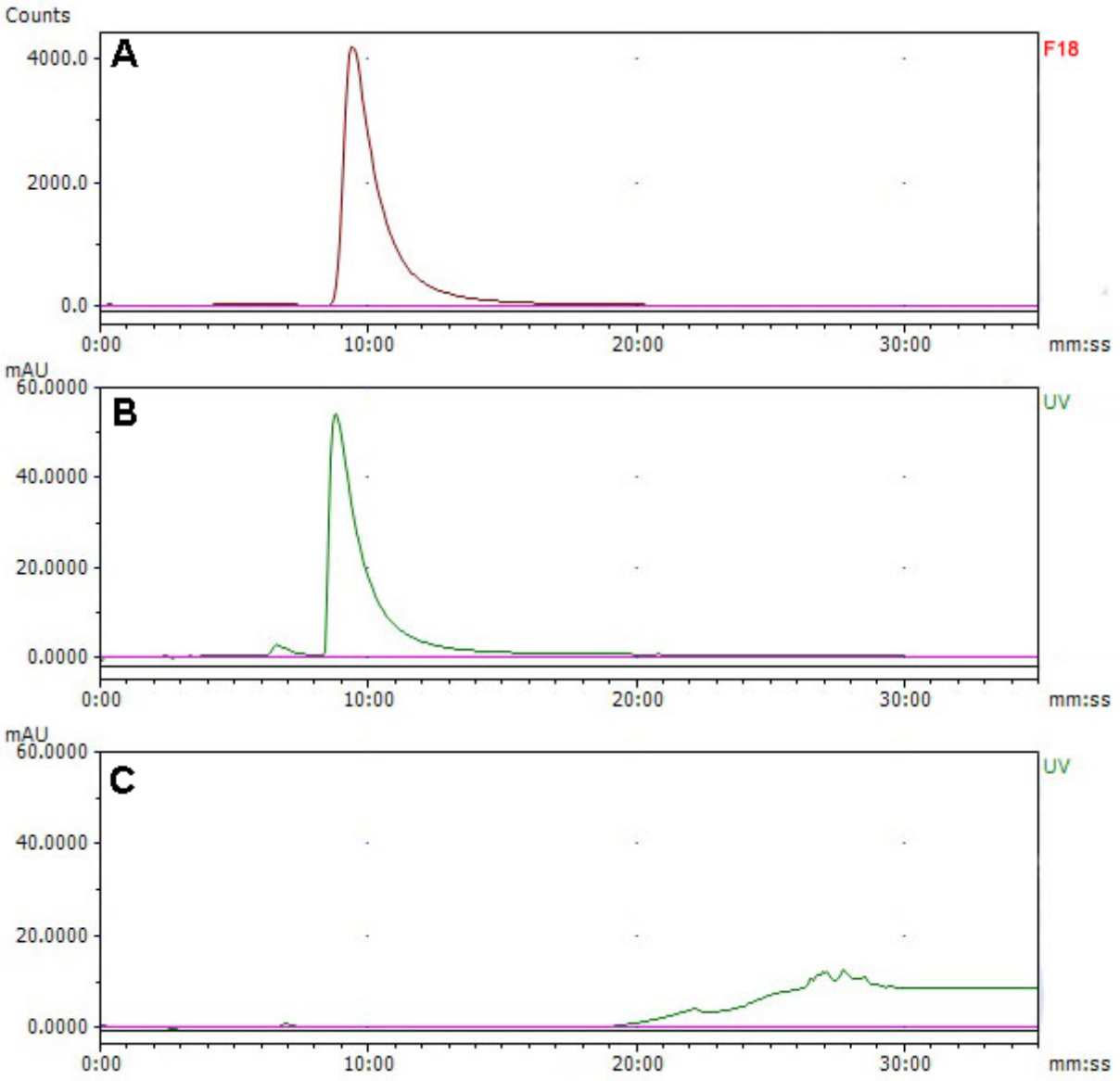

Figure 2

The Identity of 18F-deoxy-thiamine and The Measurements of Radioactivity Purity and Specific Activity. A and B: results of coinjection of 18F-deoxy-thiamine with cold standard sample. A was the radio-signal, and the retention time was 9 mins 24 secs; B was the UV-signal, and the retention time was 8 mins 47 secs. Radio-signal acquisition system was installed behind UV-signal acquisition system, and the time-lag was about half-minute at the flow rate of 0.8ml/min. Note that the peak shapes of A and B were the same. C: the UV signal of 18F-deoxy-thiamine. UV=254nm.

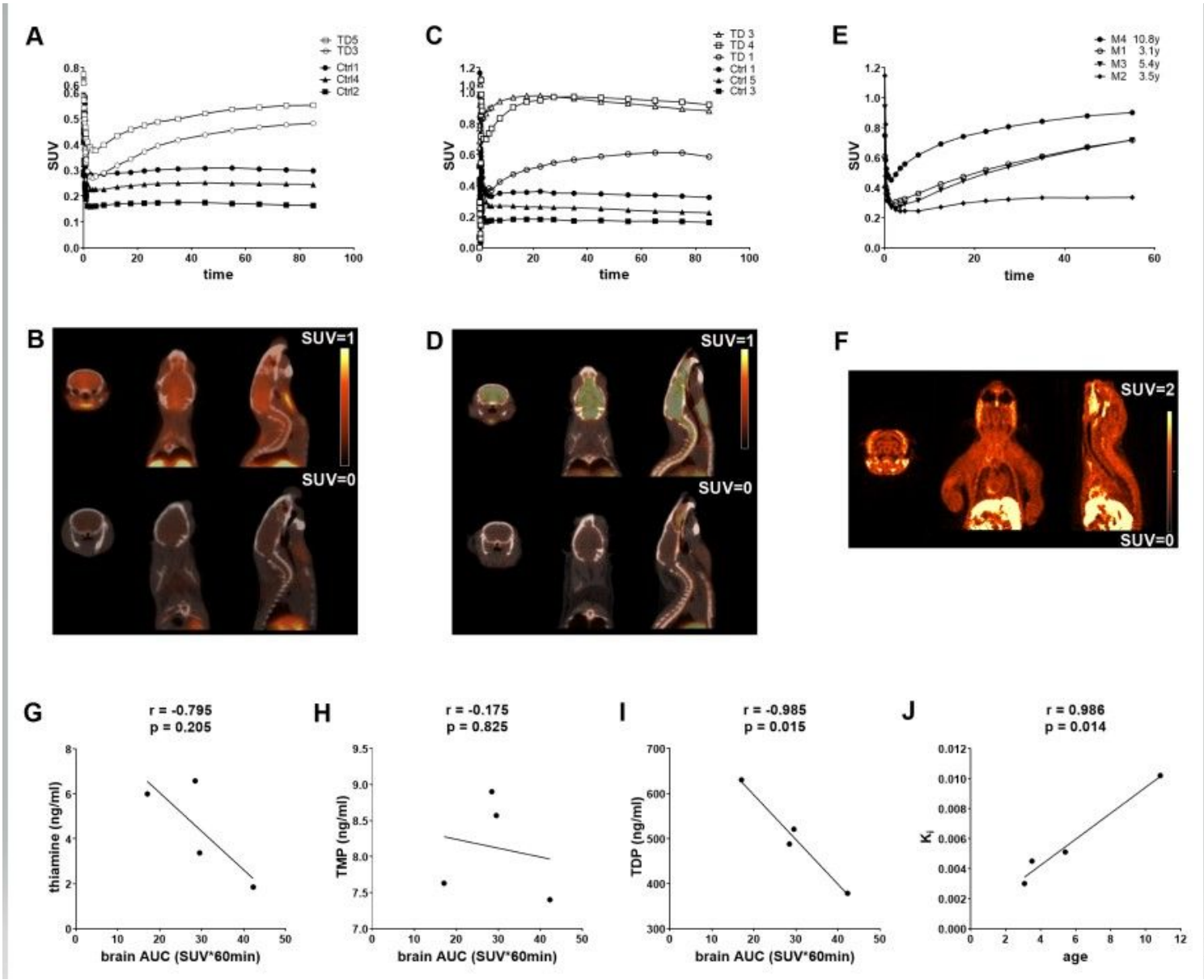

Figure 3

The Evaluation of Cerebral Thiamine Metabolism Status in Mice and Marmosets. A-B: C57BL/6 mice. A: the cerebral TACs of 18F-deoxy-thiamine in 90 mins. The average AUC value in two mice with TD was 1.9 times higher than that in control mice (38.73±3.74 vs. 20.38±3.23). B: The representative PET/CT images in TD and control groups (TD 5 and Ctrl 2, both at 50-60 min). C-D: ICR mice. C: the cerebral TACs of 18F-deoxy-thiamine in 90 mins. The AUC values in mice with TD were significantly higher than those in controls (68.28±10.74 vs. 21.88±4.25, P=0.016). D: The representative PET/CT images in TD and control mice (TD 4 and Ctrl 1, 50-60min). E-J: marmosets. E: the cerebral TACs of 18F-deoxy-thiamine in 60 mins. F: the representative PET/CT images (M4, 30-60min). G, H, I: the correlations between cerebral AUC values of 18F-deoxy-thiamine within 60 mins and blood levels of thiamine, TMP, and TDP. J: the correlation between cerebral transfer constant Ki and age.

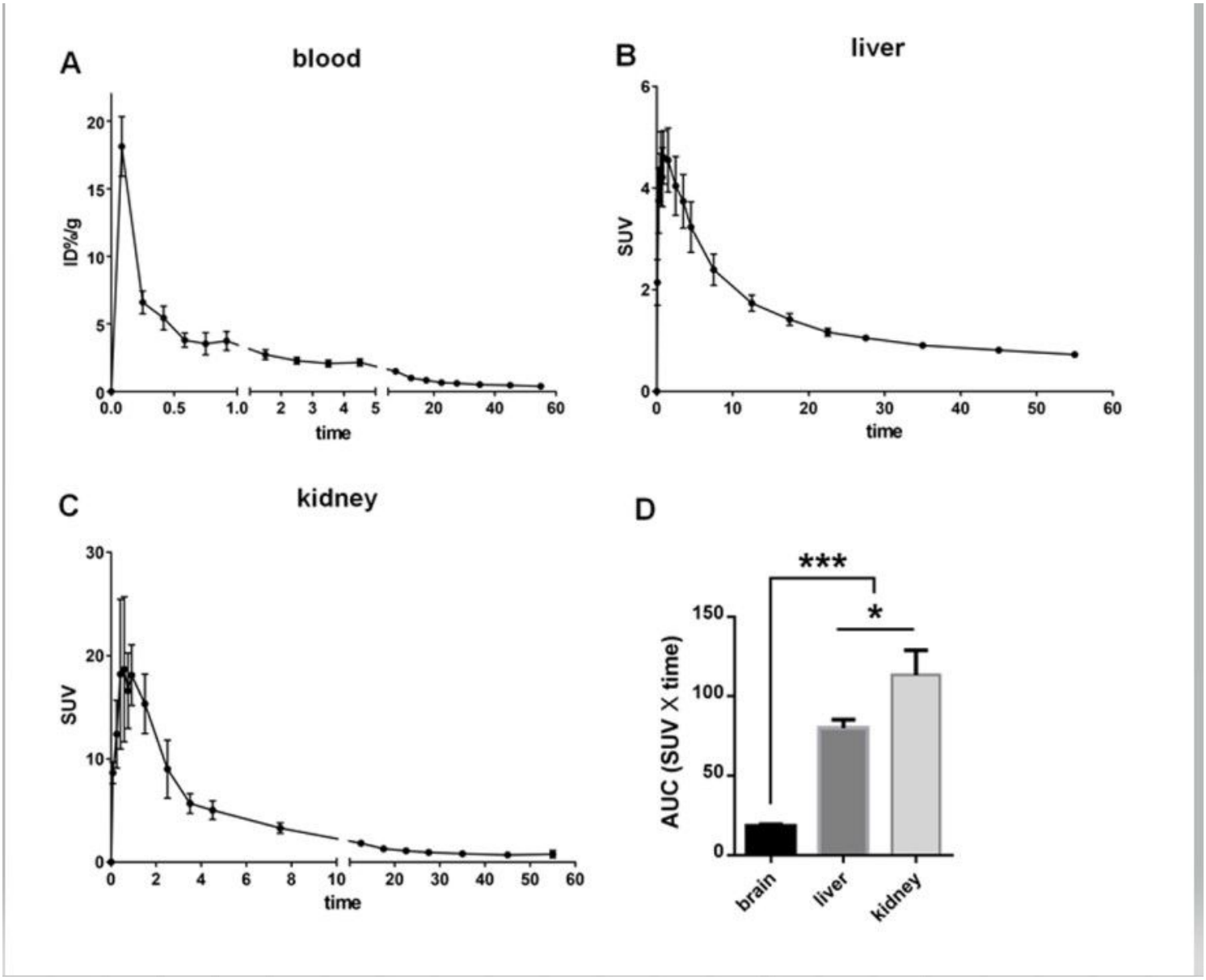

Figure 4

Studies of Pharmacokinetics and Metabolic Kinetics of 18F-deoxy-thiamine in ICR Mice. A: The TAC of 18F-deoxy-thiamine in blood (radioactivity expressed as IA%/g). B and C: the TACs of 18F-deoxy-thiamine in liver and kidney, respectively (radioactivity expressed as SUV). D. Comparisons of AUC values within 60min between brain, liver and kidney. Note that the scale of X axes in A and C was changed properly. *, $P<0.05$. ***, $P<0.001$. repeated measurement of ANOVA with Trukey's post-hoc, n=5 for each graph.

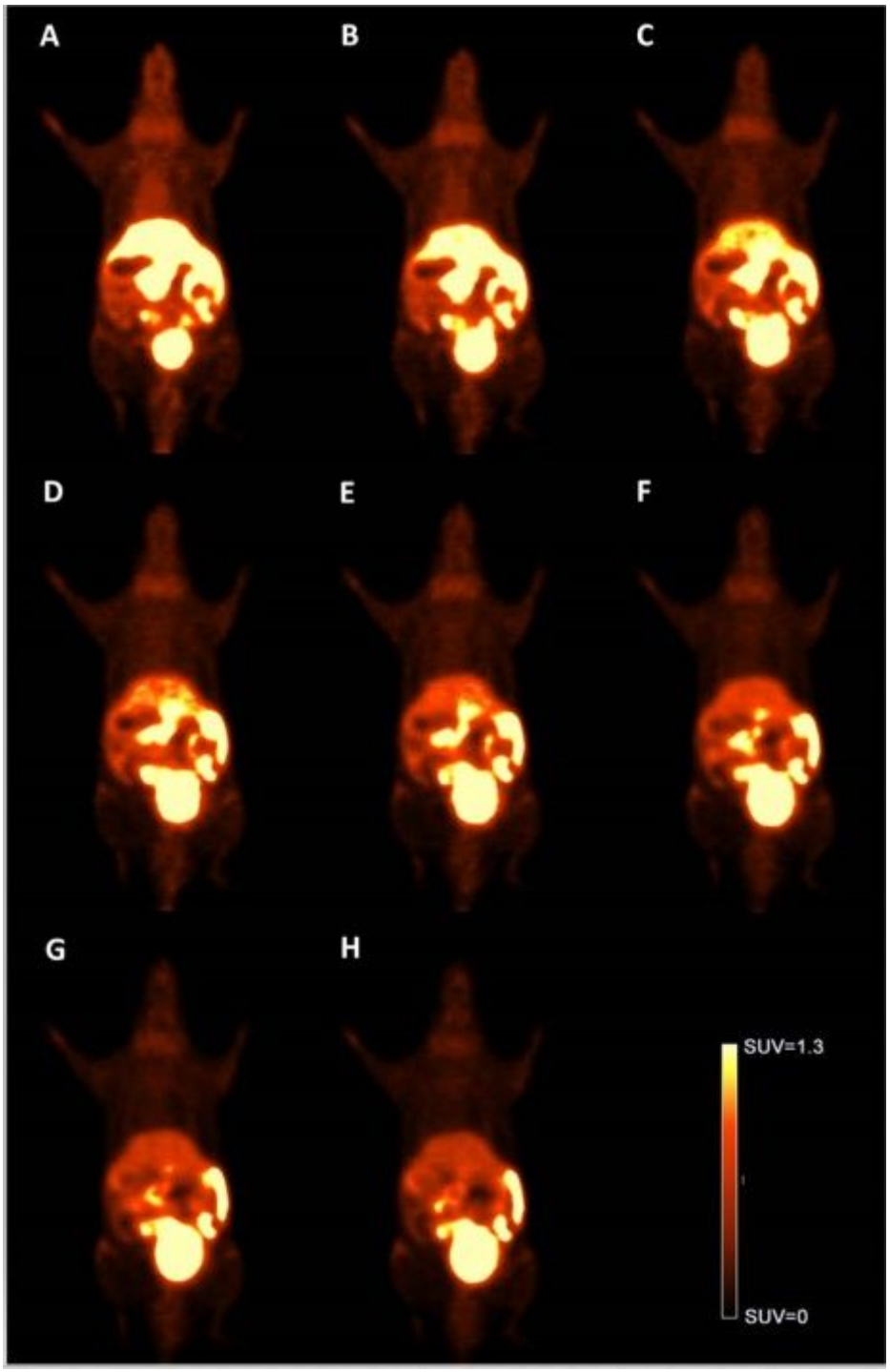

Figure 5

Dynamic Micro-PET/CT Scanning within 60 Mins The representative results from one ICR mouse. A. the 11th frame (5-10min). B. the 12th frame (10-15min). C. the 13th frame (15-20min). D. the 14th frame (20-25min). E. the 15th frame (25-30min). F. the 16th frame (30-40min). G. the 17th frame (40-50min). H. the 18th frame (50-60min).

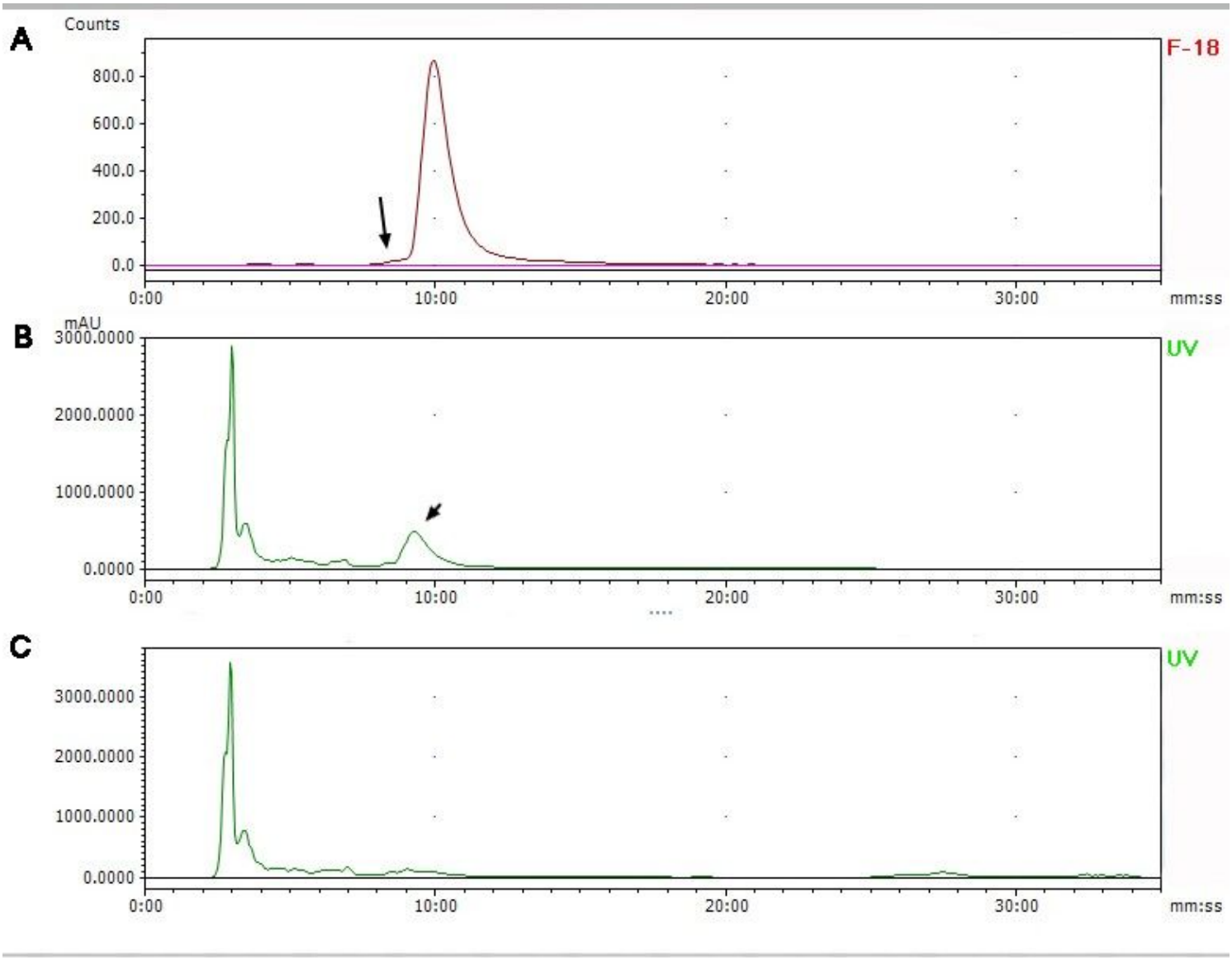

Figure 6

The Representative results of In Vivo Stability Study on 18F-deoxy-thiamine. A and B: HPLC results for the mixture of mouse urine extracts and cold standard sample of 18F-deoxy-thiamine. A: the radio-signal, and the retention time of 18F-deoxy-thiamine was 9 mins 54 secs. Note that the unknown metabolite(s) was ahead of 18F-deoxy-thiamine (arrow). B: the UV-signal, and the retention time of cold standard sample was 9 mins 14 secs (arrowhead). The UV-signal acquisition system was ahead of radio-signal and the time-lag was about half-minute. C: The UV signal of analyzing only the mouse urine extracts. UV=254nm. The peak around 3 min in B and C was the metabolic compounds excreted through kidney into urine. Although the urine was treated by deproteinization, centrifugation, and filtration, many in-vivo metabolic compounds could not be separated and removed.

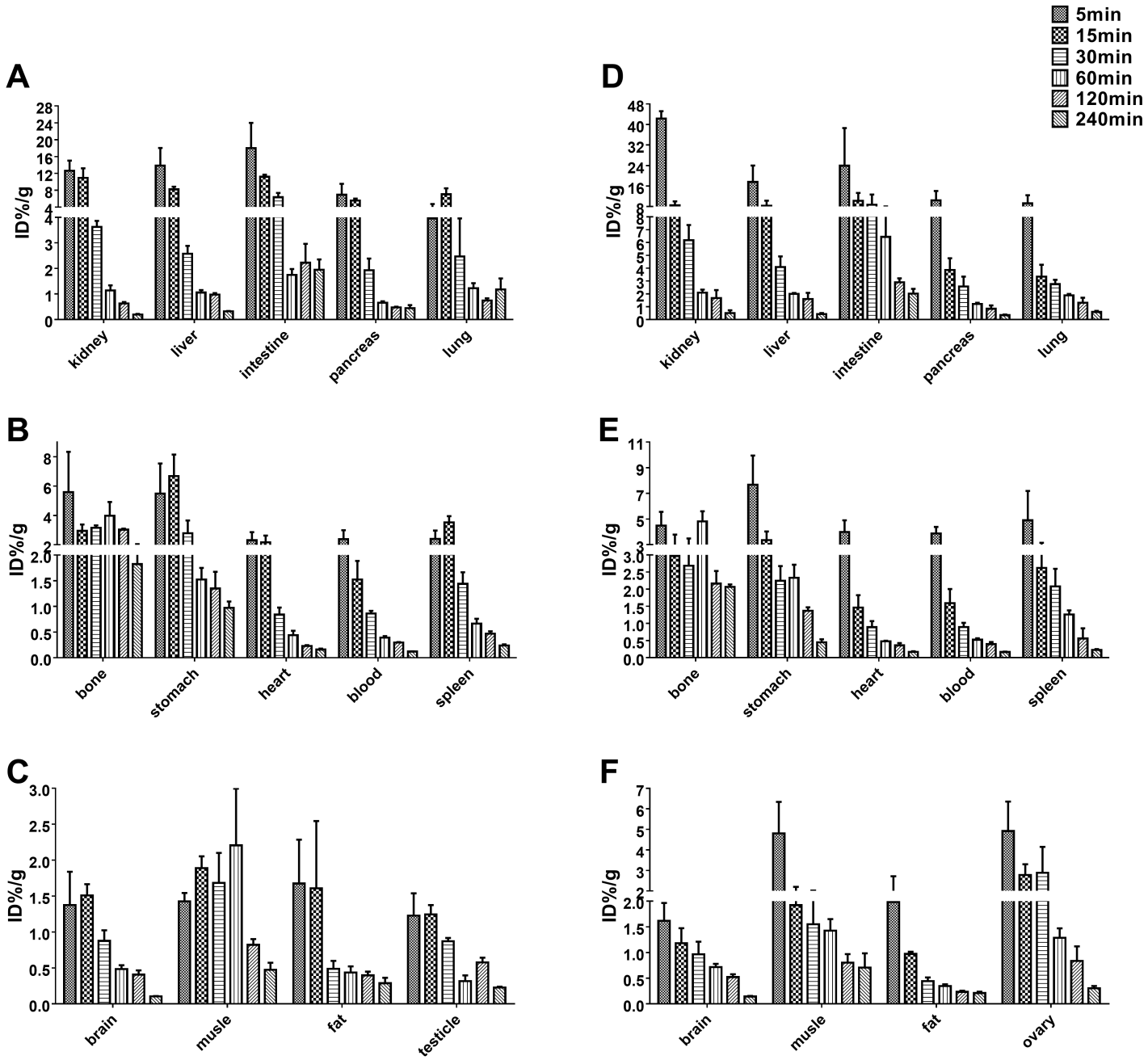

Figure 7

Biodistribution of 18F-deoxy-thiamine in ICR Mice A-C: male. D-F: female. Radioactivity accumulation was expressed as %IA/g at 5, 15, 30, 60, 120, 240 min after tail-vein injection of 3.7 MBq 18F-deoxy-thiamine in 0.1 ml volume. n=3 for each organ or tissue at eact time point, cxcept for kidney, lung at 5min of male, and kidney, liver, duodenum, lung, ovary at 5min of female (n=2).

Supplementary Files

This is a list of supplementary files associated with this preprint. Click to download.

- SuppFig3B.pdf
- supplementarytextcleanversion.docx
- SuppFig3D.pdf
- SuppFig2.tif
- SuppFig3E.jpg
- SuppFig3F.pdf
- SuppFig3C.jpg
- SuppFig3A.jpg
- SuppFig3G.jpg
- SuppFig7.tif
- SuppFig1.tif
- SuppFig4.tif
- SuppFig5.tif
- SuppFig6.tif